# Autoantibodies Against the Exocrine Pancreas in Autoimmune Pancreatitis: Gene and Protein Expression Profiling and Immunoassays Identify Pancreatic Enzymes as a Major Target of the Inflammatory Process

J.-Matthias Löhr, MD[1,2,3,19], Ralf Faissner, PhD[1,19], Dirk Koczan, PhD[4,19], Peter Bewerunge, PhD[5,19], Claudio Bassi, MD[6], Benedikt Brors, PhD[5], Roland Eils, PhD[5], Luca Frulloni, MD[6], Anette Funk, BS[1,2], Walter Halangk, MD[7], Ralf Jesnowski, PhD[1,2], Lars Kaderali, PhD[5], Jörg Kleeff, MD[8], Burkhard Krüger, PhD[9], Markus M. Lerch, MD[10], Ralf Lösel, PhD[11], Mauro Magnani, PhD[12], Michael Neumaier, MD[13], Stephanie Nittka, MD[13], Miklós Sahin-Tóth, PhD[14], Julian Sänger, MD[1], Sonja Serafini, PhD[12], Martina Schnölzer, PhD[15], Hermann-Josef Thierse, MD[16], Silke Wandschneider, PhD[1,15], Giuseppe Zamboni, MD[17] and Günter Klöppel, MD[18]

OBJECTIVES: **Autoimmune pancreatitis (AIP) is thought to be an immune-mediated inflammatory process, directed against the epithelial components of the pancreas. The objective was to identify novel markers of disease and to unravel the pathogenesis of AIP.**

METHODS: **To explore key targets of the inflammatory process, we analyzed the expression of proteins at the RNA and protein level using genomics and proteomics, immunohistochemistry, western blot, and immunoassay. An animal model of AIP with LP-BM5 murine leukemia virus-infected mice was studied in parallel. RNA microarrays of pancreatic tissue from 12 patients with AIP were compared with those of 8 patients with non-AIP chronic pancreatitis.**

RESULTS: **Expression profiling showed 272 upregulated genes, including those encoding for immunoglobulins, chemokines and their receptors, and 86 downregulated genes, including those for pancreatic proteases such as three trypsinogen isoforms. Protein profiling showed that the expression of trypsinogens and other pancreatic enzymes was greatly reduced. Immunohistochemistry showed a near-loss of trypsin-positive acinar cells, which was also confirmed by western blotting. The serum of AIP patients contained high titers of autoantibodies against the trypsinogens PRSS1 and PRSS2 but not against PRSS3. In addition, there were autoantibodies against the trypsin inhibitor PSTI (the product of the *SPINK1* gene). In the pancreas of AIP animals, we found similar protein patterns and a reduction in trypsinogen.**

CONCLUSIONS: **These data indicate that the immune-mediated process characterizing AIP involves pancreatic acinar cells and their secretory enzymes such as trypsin isoforms. Demonstration of trypsinogen autoantibodies may be helpful for the diagnosis of AIP.**

**SUPPLEMENTARY MATERIAL** is linked to the online version of the paper at http://www.nature.com/ajg

*Am J Gastroenterol* 2010; 105:2060–2071; doi:10.1038/ajg.2010.141; published online 20 April 2010

[1]Molecular Gastroenterology, German Cancer Research Center, Heidelberg, Germany; [2]Department of Medicine II, University of Heidelberg, Heidelberg, Germany; [3]Department of Surgical Gastroenterology, Karolinska Institute, Stockholm, Sweden; [4]Department of Immunology, University of Rostock, Rostock, Germany; [5]Department of Theoretical Bioinformatics, German Cancer Research Center, Heidelberg, Germany; [6]Department of Biomedical and Surgical Sciences, University of Verona, Verona, Italy; [7]Department of Surgery, University of Magdeburg, Magdeburg, Germany; [8]Department of Surgery, University of Heidelberg, Heidelberg, Germany; [9]Department of Pathology, University of Rostock, Rostock, Germany; [10]Department of Medicine A, University of Greifswald, Greifswald, Germany; [11]Department of Clinical Pharmacology, University of Heidelberg, Heidelberg, Germany; [12]Institute of Biological Chemistry, University of Urbino, Urbino, Italy; [13]Department of Clinical Chemistry, University of Heidelberg, Heidelberg, Germany; [14]Department of Molecular and Cell Biology, Boston University, Boston, Massachusetts, USA; [15]Functional Proteome Analysis, German Cancer Research Center, Heidelberg, Germany; [16]Department of Dermatology, Medical Faculty Mannheim, University of Heidelberg, Heidelberg, Germany; [17]Department of Pathology, University of Verona, Verona, Italy; [18]Department of Pathology, University of Kiel, Kiel, Germany; [19]These authors contributed equally. **Correspondence:** J.-Matthias Löhr, MD, Department of Surgical Gastroenterology, Karolinska Institutet, CLINTEC, K53, Hälsovägen, Stockholm SE-141 86, Sweden. E-mail: matthias.lohr@ki.se
**Received 20 October 2009; accepted 1 March 2010**

## INTRODUCTION

Autoimmune pancreatitis (AIP) is a unique disease within the spectrum of inflammatory changes of the pancreas (1,2). Despite great efforts, it remains a big challenge to establish its diagnosis (3). The clinicopathologic features are suggestive of an immune-related etiopathogenesis (1,2). This assumption is supported by the histopathological features of the disease (4–6), its frequent association with other autoimmune disorders (6,7), the demonstration of autoantibodies, (8,9) and the response to steroid treatment (10,11). Moreover, thymectomized mice immunized with carboanhydrase-II or lactoferrin develop a disease that closely resembles AIP (12). Circulating antibodies in AIP include autoantibodies against carboanhydrase-II, lactoferrin, and nuclear and smooth muscle antigens (ANA, ASMA) (8,9). High serum immunoglobulin (Ig) levels were already reported 50 years ago in the initial description of AIP (13). Elevated IgG4 levels are currently regarded as the most sensitive serum parameter for diagnosing AIP (14,15) and increased numbers of IgG4-positive plasma cells help to establish the histopathological diagnosis (16). To further identify the key proteins targeted by the inflammatory process in AIP, particularly those that may be indicative of an involvement of the acinar cells, we searched for related changes in the RNA and protein expression profiles of pancreatic tissue from AIP patients and compared them with those from specimens of patients with non-AIP chronic pancreatitis (non-AIP CP). We found a severe downregulation, both at the RNA and protein level of pancreatic proteases, especially trypsinogens, that was associated with a reduction in the acinar cell numbers in AIP tissues. We were able to corroborate these findings in an experimental mouse model of AIP (17). In addition, we detected high-titer autoantibodies against trypsinogensin patients with AIP.

## METHODS

### Tissue and serum samples

Human pancreatic tissue samples ($n=22$) were obtained during surgery, immediately snap frozen, and stored in liquid nitrogen. The samples were obtained consecutively, however, only tissue with approved preservation was taken. Additional samples from the same tissues were fixed in formalin and embedded in paraffin. The diagnosis of AIP ($n=12$) or non-AIP CP ($n=8$) was based on established histopathological criteria (5). The pancreas from two healthy organ donors served as controls. Patient characteristics are listed in **Supplementary Table S1** online. In addition, serum samples from 19 AIP patients (58% male, mean age: 46 years), and 23 non-AIP CP patients (78% male, mean age: 48 years), and 121 healthy subjects (49% male, mean age: 28 years) were collected. In eight patients, the diagnosis of AIP was based on the histopathological findings in the resection specimens (5). In the remaining 11 patients, the HiSORT criteria were applied (7) that allowed to establish the diagnosis of AIP based on a positive fine needle biopsy (six patients) (18), an association with other autoimmune diseases (five patients), radiological findings, and response to steroid therapy (all patients). Of the non-AIP CP patients, 18/23 had a history of alcohol abuse and 5/23 an idiopathic or hereditary pancreatitis. CP was diagnosed at least 3 years before taking the samples. Eight patients underwent pancreatic surgery (7/23 with pancreatic head resection and 1/23 with left sided pancreas resection), whose indication was either pain (4/23), pseudocyst (1/23), or stenosis of the bile duct (3/23). The local institutional review boards at the University of Heidelberg, Germany, the University of Kiel, Germany, and the University of Verona, Italy, approved the project. Written informed consent was obtained before the procurement of the biological samples.

From C57BL/6 mice infected with the murine leukemia retrovirus LP-BM5, (19) which developed symptoms and histological findings similar to human AIP (17), fresh-frozen pancreatic tissue samples ($n=6$) were obtained. Pancreatic tissues ($n=6$) from non-infected mice served as controls.

### Microarray gene expression profiling

Total RNA was prepared from human pancreatic tissue using commercially available systems (RNeasy kit, Qiagen, Hilden, Germany). Tissue was taken from the same specimen piece as for proteome analysis. RNA samples were labeled according to the supplier's instructions (Affymetrix, Santa Clara, CA) and hybridized overnight (45 °C) to HG U133A arrays (22,283 probe sets, Affymetrix) and scanned (GeneArray Scanner 2500, Hewlett Packard, Palo Alto, CA). The microarray data are deposited at ArrayExpress (http://www.ebi.ac.uk/arrayexpress/) under the entry name E-MEXP-804.

### Analysis of microarray data

Data normalization was performed by vsn (20) using CEL (Celera) intensity files. Significance analysis of microarrays (21) was used on the vsn-transformed data for calculating *P* values. Genes with a fold change $>2$ or $<-2$ and a *P* value $<0.05$ were considered to be significantly altered between AIP and non-AIP CP (**Supplementary Table S4**). Two-dimensional hierarchical cluster analysis was carried out with the differentially regulated genes. The clustering was done for the Manhattan distance in combination with the complete linkage algorithm (22).

Using the Gene Ontology (GO) database (http://www.geneontology.org), we chose a minimum similarity depth of eight for visualization of gene distances in functional GO annotation. All genes were represented by nodes in the resulting graph, and the edges connecting the two nodes were being compared. The Bioconductor package GOstats was used to calculate the distances in similarity depth (http://www.bioconductor.org). Visualization of the graph was done with Cytoscape (http://www.cytoscape.org). Function and pathway analyses were performed using the database for annotation, visualization, and integrated discovery (DAVID) platform (23).

### Proteome analysis

Proteins were extracted using a procedure described by Klose (24) modified for pancreatic specimens (25) by addition of protease inhibitors (Complete Mini EDTA-free (Roche Applied Science, Mannheim, Germany), pepstatin, phenylmethylsulphonyl fluoride). Samples for differential in-gel electrophoresis (DIGE) analysis were labeled with CyDye DIGE fluor minimal dyes (Amersham

**Table 1. List of differentially regulated proteins in autoimmune pancreatitis (AIP)**

| Protein name | Acc. no. | fc (AIP/non-AIP CP) | fc (AIP/NC) | fc (non-AIP CP/NC) |
|---|---|---|---|---|
| *Upregulated exclusively in AIP* | | | | |
| Peroxiredoxin 2 | P32119 | 2 Up | 2 Up | n.c. |
| *Downregulated exclusively in AIP* | | | | |
| Annexin A4 | P09525 | 4 Down | 4 Down | n.c. |
| Cationic trypsinogen | P07477 | 8 Down | 8 Down | n.c. |
| Anionic trypsinogen | P07478 | 6 Down | 6 Down | n.c. |
| Trypsin 3 precursor (mesotrypsinogen) | P35030 | >20 Down | >20 Down | n.c. |
| *Upregulated in AIP and non-AIP CP* | | | | |
| Serum albumin (multiple spots; isoforms / fragm.) | P02768 | n.c. | ~10 Up | ~10 Up |
| Apolipoprotein A1 (chain A) | P02647 | n.c. | 8 Up | 8 Up |
| Macrophage capping protein | P40121 | 2 Up | 5 Up | 2 Up |
| Cathepsin D (heavy chain) | P07339 | 3 Up | 5 Up | 2 Up |
| Coactosin-like protein | Q14019 | 3 Up | Not found in NC | Not found in NC |
| Pyruvate kinase, isozymes M1/M2 (fragm.) | P14618 | n.c. | 2 Up | 2 Up |
| Thymidine phosphorylase precursor (platelet-derived endothelial cell growth factor) | P19971 | 2 Up | 11 Up | 5 Up |
| Ubiquitin carboxyl-terminal esterase L1 (ubiquitin thiolesterase) | P09936 | n.c. | 7 Up | 5 Up |
| Vitamin D-binding protein precursor (2 spots) | P02774 | 2 Down | 5 Up | 10 Up |
| *Downregulated in AIP and non-AIP CP* | | | | |
| Calreticulin precursor | P27797 | Only in NC | Only in NC | Only in NC |
| Chymotrypsinogen B | P17538 | 2 Down | 4 Down | 2 Down |
| (Pro)elastase 3B (protease E) | P08861 | 6 Down | 12 Down | 2 Down |
| Pancreatic lipase-related protein 1 | P54315 | 5 Down | >20 Down | 4 Down |
| Protein disulfide isomerase precursor (fragm.) | P07237 | 2 Down | 6 Down | 3 Down |
| Protein disulfide-isomerase (P4HB protein fragment) | Q96C96 | n.c. | 6 Down | 6 Down |
| Regenerating protein 1 α (multiple spots) | P05451 | non-AIP CP>AIP | NC≫AIP | NC>non-AIP CP |
| Regenerating protein 1 β (multiple spots) | P48304 | non-AIP CP>AIP | NC≫AIP | NC≫non-AIP CP |
| MAWD-binding protein | P30039 | 2 Down | 5 Down | 3 Down |

CP, chronic pancreatitis; fc, fold change; fragm., fragmented protein; MAWD, MAP (mitogen-activated protein) kinase activator of WD (amino acids tryptophan and aspartate) repeats; n.c., not changed; NC, normal control.

Biosciences, Freiburg, Germany). Samples were loaded into linear immobilized pH gradient (IPG) strips (Immobiline DryStrips pH 4–7; Amersham Biosciences) using 75μg total protein/strip. Isoelectric focusing was performed on an IPGphor unit (Amersham Biosciences) for a total of 125kVh. Before second dimension separation, proteins were reduced by dithiothreitol and alkylated by iodoacetamide. SDS–PAGE was performed on 12.5% polyacrylamide gels running on a vertical Hoefer DALT Electrophoresis Tank (Amersham Biosciences) (25). Each sample was run at least three times to diminish experimental variability, to monitor the reproducibility, and to check the integrity of the frozen tissue samples.

The separated proteins were visualized by modified silver staining compatible with MALDI-TOF-MS (Matrix Assisted Laser Desorption Ionization - Time Of Flight Mass Spectrometry) (26) or by fluorescence laser scanning (FLA-5100 imaging system; Fujifilm Europe, Düsseldorf, Germany) according to the wavelengths of the CyDye. Silver-stained gels were digitized using a GS-800 densitometer (Bio-Rad, Munich, Germany) and imported into a two-dimensional gel image analysis program. PDQuest 7.1 (Bio-Rad) and Delta two-dimensional 3.4 (for DIGE analysis; Decodon, Greifswald, Germany) were used to locate and quantify protein spots and match spots through the gels. The statistical comparison of individual protein abundances was performed with Student's *t*-test within the software programs. Experimental $M_w$ and *pI* values were calculated internally. Proteins that showed variable changes or were present only in some of the gels were not reported.

### Protein identification by MALDI-TOF-MS

Silver or fluor-stained gel pieces were excised manually or by an automated spotpicker (Bruker Daltonics, Bremen, Germany) and subjected to in-gel digestion. Proteins were reduced, alkylated, and digested with sequencing-grade-modified trypsin (Promega,

Mannheim, Germany) as described (27). Tryptically digested protein samples were analyzed with MALDI-MS in the positive ion mode (Autoflex II time-of-flight instrument, Bruker Daltonics). Tryptic, monoisotopic peptide masses were run against the NCBInr or SwissProt nonredundant protein sequence database (Mascot; Matrix Science, London, UK) using the peptide mass fingerprint method. Identification was based on a significant Mascot score ($P<0.05$) and, in most cases, on at least five matching peptides with a protein sequence coverage of >20%. The experimental $M_w$ and *pI* values determined from the protein pattern had to be in agreement with the theoretical value of the identified proteins.

### Immunohistochemistry

Formalin-fixed pancreatic tissue from 20 patients was cut into 2 µm sections and stained with an anti-trypsin monoclonal antibody (Ventrex Laboratories, Portland, OR; 1:100), and polyclonal antibodies against cleaved caspase 3 (Santa Cruz Biotechnology, Santa Cruz, CA: 1:100). Antigen retrieval was performed for 2 min 45 sec in a pressure cooker with citrate buffer. The immunostaining was carried out using the avidin–biotin–peroxidase complex method. Apoptotic cells were defined on the basis of cell shrinkage, nuclear chromatin condensation, and fragmentation.

### Western blot

Protein samples from the same specimens as used for proteomics were subjected to 1D gel electrophoresis and blotted as described before (28). Depending on the antibodies used subsequently, lysates were mixed with either reducing or nonreducing SDS sample buffer and boiled for 5 min. Equal protein amounts were separated by SDS–PAGE and transferred into a PVDF membrane (polyvinylidene fluoride, Roche) using standard protocols (28). Blot membranes were blocked in Tris-buffered saline (10 mM Tris, 10 mM NaCl) containing 5% nonfat dry milk (New England Biolabs, Frankfurt/a M, Germany) and probed with the respective antibodies. The following antibodies were used: trypsin (H-101, rabbit polyclonal, 1:2,000, Santa Cruz, Heidelberg, Germany), trypsin 1/PRSS1 (MAB3848, mouse monoclonal, 1:250, R&D Systems, Wiesbaden, Germany), trypsin 2/PRSS2 (MAB3586, mouse monoclonal, 1:500, R&D Systems), β-actin (AC-15, mouse monoclonal, 1:10,000, Sigma, Munich, Germany), and actin (A-2066, rabbit polyclonal, 1:1,000, Sigma). Goat anti-mouse HRP and goat anti-rabbit HRP (1:5,000, both from Pierce, Bonn, Germany) were used as detection antibodies. SuperSignal West Femto Maximum Sensitivity Substrate (Pierce) was used for visualization.

### Serum trypsinogen immunoassay

The serum concentrations of anionic trypsinogen (PRSS2) were determined with a two-site noncompetitive sandwich immunoassay. Mouse monoclonal antibody specific to PRSS2 was purified with sepharose protein A and used as the primary "capture" antibody, whereas the secondary antibody was a rabbit polyclonal antibody. Antibodies were isolated from animals repeatedly immunized against PRSS2. PRSS2 was purified from human pancreatic juice by affinity and ionic exchange chromatography. Wells of microtiter plates were coated with capture mAb (10 µg/ml) in bicarbonate buffer (0.1 M, pH 9.6) overnight at 4 °C. Diluted human serum (1:400) and PRSS2 standards were added to precoated wells in triplicates. Secondary Ab was added (diluted 1:1,000 in PBS/Tween, 1 h) followed by peroxidase-conjugated anti-rabbit IgG (goat, Calbiochem, Los Angeles, CA; 1:1,000 in PBS/Tween, 30 min); 2,2′-azino-bis(3-ethylbenzthiazoline-6-sulfonic acid) (ABTS; 1.5 mM in 50 mM citrate buffer, pH 4.0, 0.007% $H_2O_2$) was used as the peroxidase substrate. The reaction was monitored at 405 nm and stopped after 10 min with oxalic acid (0.15 M).

The serum concentration of human cationic trypsinogen (PRSS1) was determined with the Elegance Neonatal IRT ELISA kit (Bioclone, Marrickville, Australia), based on specific monoclonal antibodies raised against PRSS1. A normal range of 4.2–31.5 µg/l (mean 11.5 µg/l) for serum PRSS2 and a normal range of 11.4–38.0 µg/l (mean 20.9 µg/l) for serum PRSS1 were established earlier (29).

### Serum trypsinogen and SPINK1 autoantibodies

Sandwich ELISAs were established for human IgG autoantibodies against all three trypsinogen isoforms and SPINK1. Recombinant human PRSS1 (30), PRSS2 (31), PRSS3 (32), and PSTI (33) were used. Recombinant trypsinogens (500 ng per well) and SPINK1 (400 ng), diluted in sodium carbonate buffer (Merck, Darmstadt, Germany, pH 9.6) were incubated overnight at 4 °C. Serial dilutions of human IgG (Octapharma, Langenfeld, Germany) ranging from 4 to 1,000 pg/ml were used as standards. Blocking was performed using 3% bovine serum albumin (BSA) in PBS/Tween. Sera from patients with AIP and non-AIP CP and sera from healthy blood donors were diluted 1:1,600 (trypsinogen) or 1:600 (PSTI) in PBS/Tween with 1% BSA and incubated for 2 h at 37 °C. A polyclonal goat anti-human IgG (H + L) peroxidase conjugate (1:5,000, Dianova, Hamburg, Germany) was used for the detection of bound Igs and staining with tetramethylbenzidine (TMB) substrate kit (Pierce, Rockford, IL). All samples were run in triplicate. Anti-trypsinogen IgG concentrations were normalized to total protein concentrations. The protein content was measured using a BCA assay (Perbio Science, Bonn, Germany).

### Bioinformatic analysis of serum antibody data

Logistic regression was used for pairwise separation of the three classes: AIP, non-AIP CP, and healthy controls. The models were fitted using conjugate gradient descent, with leave-one-out cross-validation for each classification pair (AIP vs. control, non-AIP CP vs. control, and AIP vs. non-AIP CP). Sensitivity, specificity, and accuracy were computed from the cross-validation runs. Mean regression coefficient values were used to analyze the significance of inputs.

## RESULTS

### Histological and immunohistochemical characterization

The pancreatic resection specimens obtained for histopathological examination and used in the RNA and protein profiling studies showed the typical features of either AIP or non-AIP CP (5,34). Briefly, in 12 specimens, dense periductal, inter lobular, and interacinar lymphoplasmacellular infiltrates were found in association with a storiform fibrosis and an obstructive phlebitis. These changes that

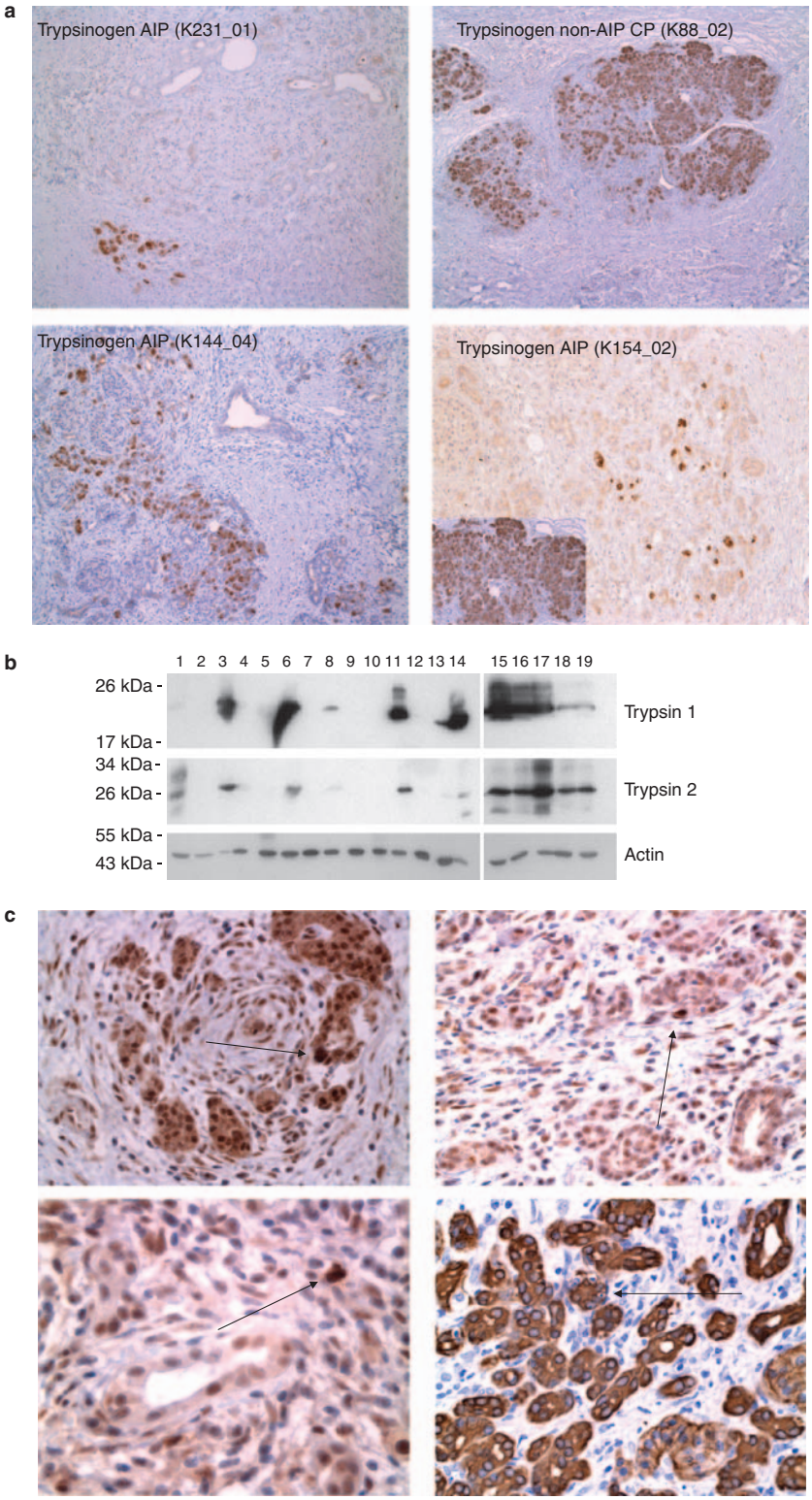


**Figure 1.** (**a**) Immunostaining for trypsinogen showed only individual positive cells in autoimmune pancreatitis (AIP) in contrast to non-AIP chronic pancreatitis (non-AIP CP) (right upper frame). Inset: trypsinogen in normal pancreas. (**b**) Western blot for trypsinogen: lanes 1–2 normal pancreas, lanes 3–14 AIP, lanes 15–19 non-AIP CP. (**c**) Immunostaining for caspase-3 identified individual positive cells in AIP. Arrows indicate apoptotic acinar cells. Right lower frame: cytokeratin 8 staining showing apoptosis in epithelial pancreatic cells. For details see "Methods."

**Table 2. List of differentially regulated proteins in C57BL/6 mice infected with LP-BM5 murine leukemia retrovirus**

| Protein name | Acc. no. | fc (infected/healthy) |
|---|---|---|
| *Upregulated in infected mice* | | |
| Albumin (fragm.) | P07724 | 1.58 |
| Chymotrypsinogen B-precursor (14 kDa fragment 1) | Q9CR35 | 1.25 |
| Chymotrypsinogen B-precursor (14 kDa fragment 2) | Q9CR35 | 1.28 |
| Glutathion-*S*-transferase pi1 | P19157 | 2.46 |
| Heat shock 70 kDa protein 5 (78 kDa glucose-regulated protein) | P20029 | 1.73 |
| Heat shock protein 9 (75 kDa glucose-regulated protein) | P38647 | 1.78 |
| Leukocyte elastase inhibitor A (serpin B1a) | Q9D154 | 1.84 |
| Peroxiredoxin 4 (fragm.) | O08807 | 1.67 |
| Peroxiredoxin 6 | O08709 | 2.26 |
| Superoxid-dismutase 1 | P08228 | 1.52 |
| Trypsinogen-8/9 (side isoform) | AAB69056 | 2.94 |
| *Downregulated in infected mice* | | |
| Apolipoprotein A-I precursor | Q00623 | 0.80 |
| Chymotrypsinogen B precursor (isoform 1) | Q9CR35 | 0.71 |
| Chymotrypsinogen B precursor (isoform 2) | Q9CR35 | 0.69 |
| (Pro)elastase 3B (isoform 1) | NP_080695 | 0.87 |
| (Pro)elastase 3B (isoform 2) | NP_080695 | 0.62 |
| Trypsinogen-8 (anionic trypsin-4 precursor) | AAB69056 | 0.40 |
| Trypsinogen-20 (anionic trypsin-2 precursor) | P07146 | 0.48 |

fc, fold change; fragm., fragmented protein.

are regarded as diagnostic of AIP (5) were focused on the pancreatic head and involved also the distal bile duct, causing its obstruction. Of the 12 cases, 8 corresponded to the lymphoplasmacytic sclerosing pancreatitis type of AIP, which had also been recently called AIP type 1 (35) and 4 showed the idiopathic duct-centric CP type of AIP or AIP type 2 (**Supplementary Table S1**). The degree of reduction of the acinar cell numbers by fibrosis was estimated semiquantitatively in sections immunostained for trypsin. In the AIP cases there was an 80–95% loss of acinar cells compared with normal pancreatic tissue (**Figure 1a**). In the few remaining acinar cells, single apoptotic figures and/or cytoplasmic immunohistochemical positivity for caspase 3 were seen (**Figure 1b**). In non-AIP CP the pancreatic changes were characterized by a patchy, predominantly interlobular fibrosis that was not as cellular as in AIP, containing only few lymphocytes, plasma cells, and macrophages. The loss of acinar cells amounted to 40–80%. Apoptotic figures and caspase 3-positive acinar cells were not observed.

### RNA expression profiles

RNA expression profiling was performed in pancreatic tissues from resection specimens of 4 of the 12 AIP and 5 of the 8 non-AIP CP patients using microarray technology. In all, 358 of the 22,283 genes were differentially expressed (**Supplementary Table S4**); 272 genes were upregulated in AIP compared with non-AIP CP, including those encoding various Igs, chemokines, major histocompatibility complex proteins, interleukin receptors, TNF receptors, CD 25, CD28, CTLA-4, Fox-P3, matrix metallopeptidases 9 and 12, S100 calcium-binding protein A8/A9 (36), granzyme, and five members of the cathepsin family (**Supplementary Table S4a**). In contrast, the expression of 86 genes, including the genes of several proteases (anionic and cationic trypsinogen, mesotrypsinogen, chymotrypsinogen, (pro)elastase), was downregulated in AIP. Furthermore, transcripts of amylase, lipase, REG1, albumin, and serine protease inhibitors were less abundant in AIP than in non-AIP CP (**Supplementary Table S4b**). The individual samples had most of the outlying genes in common. There was no difference between type 1 and type 2 AIP. Two-dimensional unsupervised hierarchical clustering showed distinct class separation of the four patients with AIP from the five with non-AIP CP (**Figure 2a**).

We used the GO Database and Kyoto Encyclopedia of Genes and Genomes pathway analysis to cluster up- and downregulated genes according to function or pathway. Analysis using a GO depth of five showed that most of the upregulated genes in AIP could be ascribed to (auto)immune responses (43%), signal transduction (34%), and apoptosis (8%). Other upregulated genes encoded for mediators in immune defense pathways and cell adhesion (26 genes), major histocompatibility complex 1, and major histocompatibility complex 2 pathways (21 genes), natural killer cell-mediated cytotoxicity (17 genes), and the T-cell receptor signaling pathway (13 genes). The 86 downregulated genes in AIP could be mapped predominantly to metabolic processes (63%). Most of these genes encoded catalytic active enzymes, especially proteases and lipases, from acinar cells.

To gain more detailed information, we performed a *visualization of distances* in functional GO annotation between the genes, because a measure of the degree of relationship can be obtained by comparing the number of nodes that two genes share on the same GO path (37,38). Calculating the relationship between the 358 differentially regulated genes showed that 79 genes had a similar depth (≥8) as at least one other gene. Thirty-three of the most differentially regulated genes (**Figure 2b**) were found to be involved in one of six biological processes: proteolysis and peptidolysis, regulation of transcription, induction of apoptosis, actin cytoskeleton organization and biogenesis, and calcium ion homeostasis.

### Protein expression profiles

In tissue samples from12 AIP and 6 non-AIP CP specimens and 14 tissue samples from two pancreas specimens from healthy subjects, there was a striking similarity of the individual protein expression patterns within the different groups and only minor interindividual differences. About 1,000–1,500 protein spots were detected on

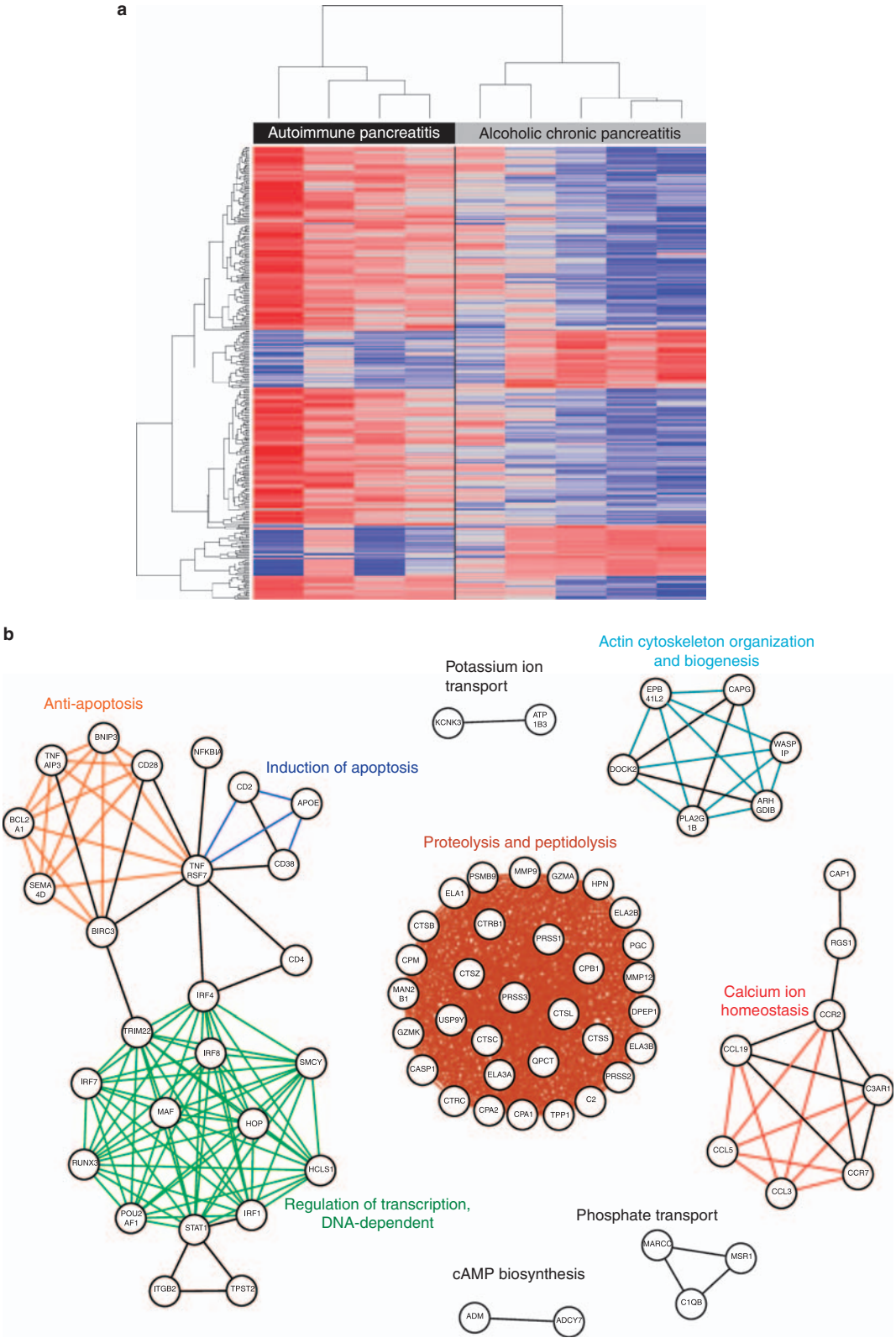


**Figure 2.** (**a**) Two-dimensional hierarchical cluster analysis of autoimmune pancreatitis (AIP) and non-AIP chronic pancreatitis showing a clear separation between the two varieties. Blue color refers to downregulation in AIP and red color to upregulation. Clustering of patients was based on 358 differentially regulated genes (for details see Methods). (**b**) Graph indicating functional relationships between differentially regulated genes based on Gene Ontology (GO) annotations. Threshold is a GO depth of ≥8. Only the 79 genes that reached or exceeded the threshold are shown. Nodes represent genes and are labeled with the HUGO symbol. Edges show the connection between the two nodes that are compared. In all, 26 different biological processes based on GO terms are represented.

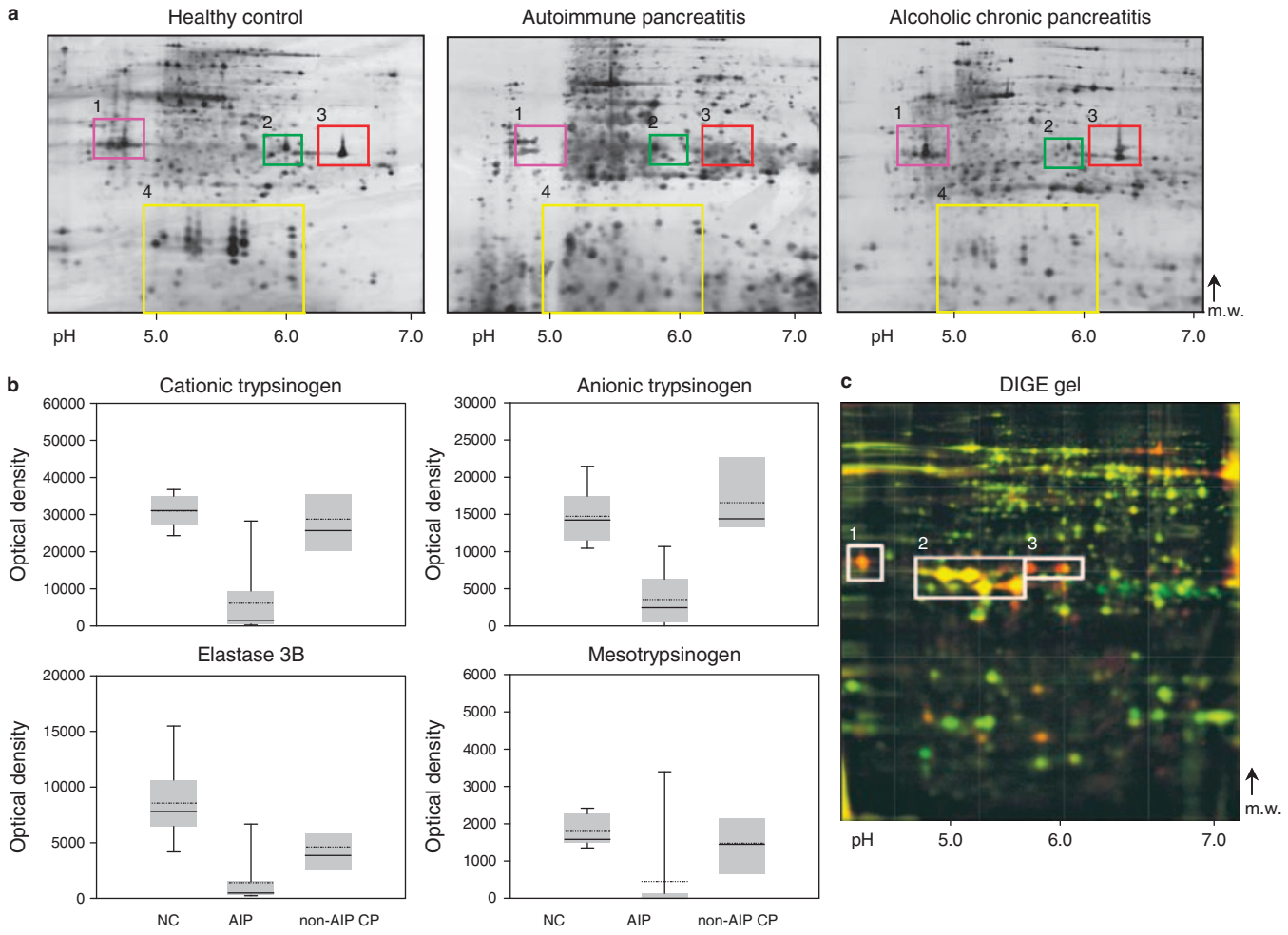


**Figure 3.** Proteome analysis. (**a**) Representative, silver-stained two-dimensional gel electrophoresis gels of human pancreas (pH 4–7). The regions with major spot intensity changes are indicated: 1: anionic trypsinogen (PRSS2); 2: (pro)elastase 3B (ELA3B) and mesotrypsinogen (PRSS3); 3: cationic trypsinogen (PRSS1); 4: regenerating protein I. (**b**) Protein levels in the tissue of autoimmune pancreatitis (AIP) patients, non-AIP CP patients, and healthy controls. The boxes indicate the median/mean and 25th/75th percentiles. Single line denotes mean and broken line the median. (**c**) Overlaid differential in-gel electrophoresis (DIGE) gel of murine pancreas; green channel: MAIDS-infected mouse; red channel: healthy mouse. The spot regions with differentially regulated proteases are indicated: 1: trypsinogen-20; 2: chymotrypsinogen B and trypsinogen-8; 3: (pro)elastase 3B. MAIDS, murine acquired immune deficiency syndrome; NC, normal control.

silver-stained two-dimensional gels. A master gel was obtained for human pancreatic tissue matching the spot data from the actual gels (**Supplementary Figure S1**). More than 100 characteristic protein spots per replicate group, present in all three groups, were picked as landmark proteins. MALDI-TOF MS identification showed a matching accuracy of nearly 100%. From these characteristic protein spots a protein database of the normal human pancreas was established (**Supplementary Figure S1**; **Supplementary Table S2**). As the AIP cases showed a distinct pattern with very little interindividual differences that showed a clear-cut separation from both non-AIP CP and normal pancreas, it was not possible to distinguish between the two subtypes of AIP on the basis of the two-dimensional protein pattern.

In a second series, samples of each tissue type were pooled to reduce individual differences. More than 20 proteins were differentially expressed to a significant degree in AIP (fold change >2, $P<0.01$). We found a significant reduction in 5 protease precursors in 11 of 12 AIP tissues. These were cationic trypsinogen (PRSS1), anionic trypsinogen (PRSS2), mesotrypsinogen (PRSS3), chymotrypsinogen B, and (pro)elastase 3B (CELA3B) (**Figure 3**). In eight samples, PRSS1, PRSS3, and CELA3B were absent or visible only in traces (<5% compared with normal pancreatic tissue), in three other samples, they were markedly reduced (25–50%). Western blot confirmed the downregulation and proper size of both PRSS1 and PRSS2 (**Figure 1a**). Non-AIP CP samples showed only a slight decline in CELA3B and no significant change in the intensity of PRSS1, PRSS2, and PRSS3.

Other changes in the protein expression patterns concerned the regenerating protein I (REG1) isoforms, whose spot pattern seen in the normal pancreas (**Figure 3a**) was absent in AIP and reduced in non-AIP CP (1–70%), and 14 further proteins that were differentially expressed in AIP exclusively or in both types of CP. The latter proteins included cathepsin D (heavy chain) and thymidine phosphorylase (platelet-derived endothelial cell

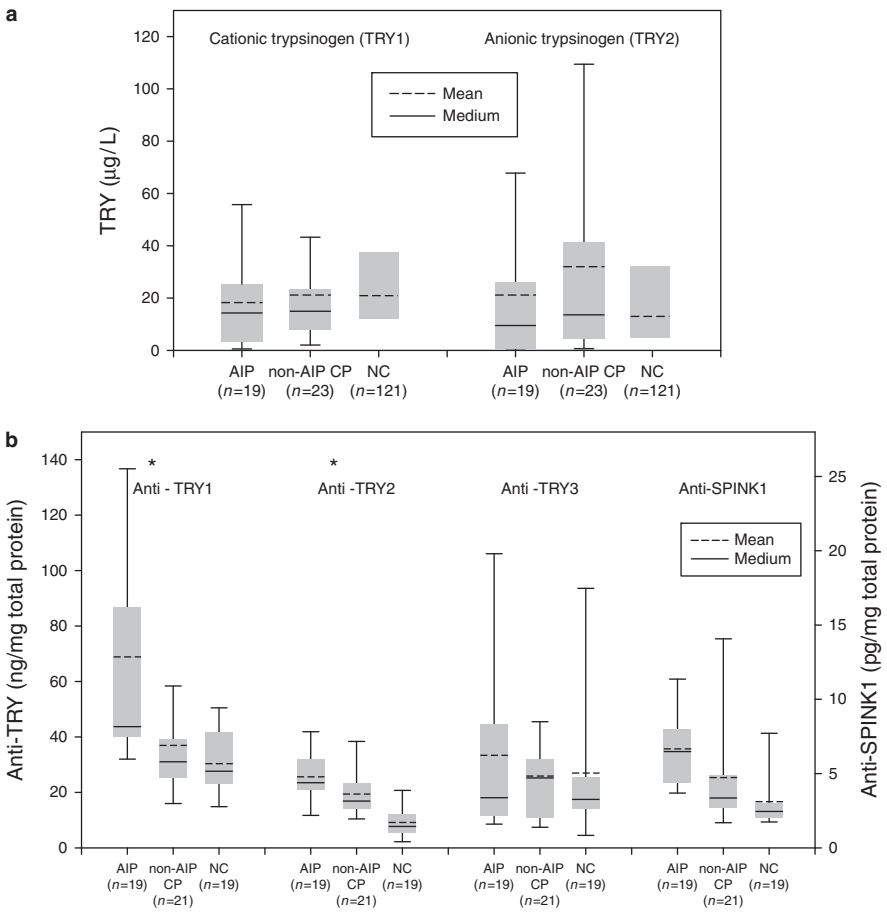


**Figure 4.** Box plot chart of serum analysis. (**a**) Serum PRSS1 and PRSS2 were not significantly affected by pancreatitis. (**b**) Elevated serum levels of anti-PRSS1, anti-PRSS2, and anti-PSTI in autoimmune pancreatitis (AIP) patients. The boxes indicate the median/mean and 25th/75th percentiles. Asterisks indicate a significant change in antibody level ($P<0.05$). NC, normal control.

growth factor), which were significantly upregulated in AIP tissues compared with the normal pancreas and non-AIP CP (**Table 1**). A selection of evaluated candidate molecules that emerged from the expression profiling (both transcriptomics and proteomics) as relevant to the pathogenesis of acute and CP and pancreatic physiology in general (39) was chosen for further analysis.

### Protein expression profiles of C57BL/6 mice

With two-dimensional differential in-gel electrophoresis (DIGE), 20 protein spots were differentially expressed in murine leukemia retrovirus LP-BM5-infected mouse pancreas (fold change >1.2, $P<0.05$) (**Figure 3c**). As in human AIP, isoforms of serine proteases (murine trypsinogen-8 and -20, chymotrypsinogen B, (pro)elastase 3B) were significantly downregulated (**Table 2** and **Supplementary Table S3**).

### Trypsinogen serum levels

As proteases were reduced at the RNA and protein level, we measured the trypsinogen concentrations in the serum of 19 patients with AIP, 23 patients with non-AIP CP, and 121 healthy subjects. This showed no significant differences between the three groups, especially for cationic (PRSS1) and anionic trypsinogen (PRSS2) (**Figure 4a**). Only the relation between PRSS1 and PRSS2, which is 1:3 in healthy individuals and inverted to 2:1 in non-AIP CP, (40) was found to be 1:2 in AIP.

### Autoantibodies against trypsinogen and SPINK1

As we found not only the ducts (9) but also the acinar tissue severely affected in AIP, we searched for autoantibodies against trypsinogen isoforms and the trypsin inhibitor PSTI in patients with AIP (data listed in **Supplementary Table S5**). We found significantly elevated levels of IgG directed against PRSS1 and PRSS2, but not PRSS3, in AIP compared with non-AIP CP and healthy subjects (**Figure 4b**). We also detected autoantibodies against PSTI in AIP (41). A logical regression analysis coupled with leave-one-out cross-validation showed that the autoantibody serum data had a predictive accuracy of 80% for distinguishing patients with AIP from those with non-AIP CP, and an accuracy of 86% for AIP patients vs. healthy controls. The sensitivity of the autoantibody test was 68% for AIP vs. non-AIP CP and 79% for AIP vs. controls. The specificity was 90% for AIP vs. non-AIP CP and 95% for AIP vs. controls (**Supplementary Table S6**).

## DISCUSSION

AIP is a disease that predominantly involves the pancreatic ducts and in many cases the bile ducts (42), with characteristic histopathology and typical changes on endoscopic retrograde cholangio-pancreatography and magnetic resonance cholangio-pancreatography. The histopathological features of AIP include a storiform fibrosis, dense periductal and also diffuse lymphoplasmacellular infiltrates, obliterative venulitis, and the presence of numerous CD4 and CD8 lymphocytes (5,8). Recently, two subtypes of AIP were described: lymphoplasmacytic sclerosing pancreatitis (also called AIP type 1) with presence of IgG4-posivite cells and idiopathic duct-centric chronic pancreatitis or AIP with so-called granulocyte-epithelial lesions (also called AIP type 2) (5,35,43). These features have raised the possibility that AIP is an immune-mediated inflammatory process. Autoantibodies against carboanhydrase-II, one of the main enzymes of bicarbonate-secreting duct cells, have been reported in AIP patients (9), and supported the notion that in AIP primarily the pancreatic duct epithelium is targeted by the immune cells (44). Our data suggest that acinar cells and their protein components also seem to be targeted by the inflammatory process. This is associated with the occurrence of autoantibodies against trypsinogens, which may be clinically useful for the diagnosis of AIP.

As we chose to analyze nonmicrodissected pancreatic tissue, a certain degree of heterogeneity among the various samples was expected. However, the two-dimensional protein patterns that we obtained from the various probes were strikingly similar. Therefore, our global RNA expression analysis showed clear differences between the AIP tissues in comparison with the non-AIP CP and normal pancreas tissues. We found 272 upregulated genes and 86 downregulated genes. Among the upregulated genes, we identified several encoding for Igs and proinflammatory as well as immunologically active chemokines and their receptors. The downregulated genes included those encoding for pancreatic proteases such as trypsinogens, chymotrypsinogen, and (pro)elastase, as well as amylase and lipase. Other downregulated genes that might also be of interest in conjunction with AIP were regenerating protein 1 (REG1/PAP), which acts anti-inflammatory (45). On the protein level, several REG1 isoforms are lacking in AIP. Low REG1 levels could, therefore, contribute to the overwhelming inflammatory infiltrate seen in AIP (5).

The profound downregulation of the genes was paralleled by a similar loss of the respective gene product. Using protein profiling either no trypsinogen and (pro)elastase 3B or only traces of them were found in 8 of 12 tissue specimens from AIP patients. In three other specimens, these proteases were reduced to 25% compared with the values observed in non-AIP CP or normal pancreatic tissues. These data suggested a severely restricted synthesis and production of proteases and other pancreatic enzymes in AIP in comparison to controls or pancreatitis of nonimmune origin. As these proteins are a product of acinar cells, we analyzed the same AIP and non-AIP CP tissues that had been analyzed for their protein profile and content, for the presence and number of acinar cells using immunohistochemical staining for trypsin that was controlled by western blotting. These analyses showed that the number of trypsin-positive acinar cells in AIP and non-AIP CP correlated with the amount of trypsin detected by protein profiling in the respective samples. Although in the AIP tissues the number of acinar cells was reduced by 80–95%, in non-AIP CP the acinar tissue compartment was only diminished by 40–60% of that of the normal pancreas. A similar reduction in acinar cell numbers and content of proteases was found in the animal model of AIP (17) that we used for comparison with human AIP. Such a significant reduction of proteases suggests that the inflammatory processes would completely and, therefore, irreversibly destroy the acinar cells in AIP. However, most AIP patients respond well to steroid therapy, and the production of digestive enzymes is restored in the acinar cells (46). Therefore, we conclude that the protease deficiency is not only a matter of a reduction in the number of acinar cells. The significant reduction might reflect the degree of inflammatory intensity that could also vary in different areas of the pancreas (5,47).

Owing to the loss of acinar cells in AIP we analyzed the serum levels of circulating trypsinogen and compared activities in AIP with those in non-AIP CP and healthy controls. These data indicate that the trypsinogen serum levels of AIP and non-AIP CP patients were both within the normal range and not affected by the acinar cell loss. An explanation for this finding could be that in most cases the patchy tissue involvement of AIP and non-AIP CP leaves enough viable acinar cells in the remaining pancreas to maintain normal serum levels of trypsin and other pancreatic enzymes. There is, however, as yet no ready explanation why the relation between cationic and anionic isoforms of trypsin (40) is changed in AIP compared with non-AIP CP.

The cause of the substantial loss of acinar cells and their replacement by fibrosis during the course of AIP is not known. In non-AIP CP caused by excessive alcohol consumption focal necrosis of the pancreatic parenchyma is followed by activation of stellate cells and myofibroblasts, which then produce extracellular matrix (48). The histopathological features of AIP suggest an immune-related attack against various cellular components of the pancreas. According to our data this attack is not only directed to the ductal cells and their components but also against the acinar cells, as we found high-titer autoantibodies against trypsinogens (PRSS1 and PRSS2) and PSTI (41) in AIP patients. As non-AIP CP patients lacked these antibodies, the development of autoantibodies against trypsinogens and the trypsin inhibitor PSTI seems to be typical for AIP. Further evidence that the proteins of the acinar cells are targeted in AIP is provided by the findings of a recent study in AIP patients showing autoantibodies against an ubiquitin subunit (UBR2), which is another particular acinar protein (49).

The initial events triggering AIP are not known. It may be speculated that the pancreatic cells are primarily injured either by a virus or by another infectious agent that causes altered cellular proteins, which, in turn, become the targets of immune-

mediated processes. Such a pathogenetic mechanism was suggested for the virus-induced AIP mouse model (17) in which we found secretory protease deficiencies strikingly similar to the situation in human AIP. Such an infection could induce a molecular mimicry that subsequently produces an autoimmune reaction—a process that has been also recently be discussed for UBR2, because it shows homology to the plasminogen-binding protein of *Helicobacter pylori* (49), which had already been suggested as a causative agent, based on a homology between the cag A and the carbonic anhydrase 2 (50). However, we could not detect *H. pylori* in the pancreas of patients with various diseases including AIP (51).

Whether in such a scenario the demonstrated autoantibodies against trypsin isoforms, PSTI and UBR2, have any significant role in the destruction of acinar cells remains to be determined. It seems, however, that the acinar cells in AIP undergo cell death through apoptosis because we found apoptotic bodies in individual cells that also stained for the apoptosis-related enzyme caspase 3 and morphologically corresponded to acinar cells.

In summary, our study shows that acinar cells, in addition to ductal cells, are target of the immune-related inflammatory process-characterizing AIP. Clinically, the loss of the acinar cells is associated with elevated antibody titers for PRSS1, PRSS2, and PSTI, The detection of these antibodies by ELISA may help to distinguish AIP from other types of pancreatitis such as alcoholic pancreatitis. It seems that the loss of acinar cells and the occurrence of autoantibodies to trypsinogens are findings typical for both subtypes of AIP, as we failed to detect any clear differences regarding these parameters between the so called subtype 1 and subtype 2 AIP.

## CONFLICT OF INTEREST

**Guarantor of the article**: J.-Matthias Löhr, MD.

**Specific author contributions:** Conceived the idea, planned the experiments, and wrote the paper: J.-Matthias Löhr; contributed patient material and clinical information: Claudio Bassi, Luca Frulloni, Jörg Kleeff, Günter Klöppel, J.-Matthias Löhr, and Guiseppe Zamboni; RNA expression profiling: Ralf Jesenofsky and Dirk Koszan; proteomics: Ralf Faissner, Anette Funk, Martina Schnölzer, Julian Sänger, Hermann-Josef Thierse, and Silke Wandschneider; bioinformatics: Peter Bewerunge, Benedikt Brors, Roland Eils, and Lars Kaderali; animal model of AIP: Mauro Magnani and Sonja Serafini; immunhistochemistry: Anette Funk and Ralf Jesenofsky; contributed purified recombinant proteases (SPINK1, TRY's): Walter Halangk and Miklós Sahin-Tóth; autoantibody ELISA: Michael Neumaier and Stephanie Nittka.

**Financial support**: This work was supported by the Federal Ministry of Education and Research (BMBF FKZ 01GG0101 and BMBF FKZ 01GR450 to J.M.L.). P.B. received a stipend from the DFG Research Training Group 886. We are grateful to Dr Patrick Pankert and Stefanie Helm (Department of Dermatology, Mannheim, Germany) for assistance and access to Delta two-dimensional software and spot picking technology, and Kay Dege for critical review.

**Potential competing interests**: None.

## Study Highlights

### WHAT IS CURRENT KNOWLEDGE

- ✓ Autoimmune pancreatitis (AIP) is an inflammatory disease of the exocrine pancreas with the features of an immune-mediated process.
- ✓ Elevated serum levels of IgG and IgG4 are of diagnostic relevance, in many (up to 50%) but not all patients.
- ✓ Autoantibodies against ductal antigens (carbonic anhydrase 2, lactoferrin) have been described earlier.
- ✓ Recently, autoantibodies against UBR2, an acinar protein, have been reported.
- ✓ Diagnosis is difficult to establish in a significant proportion of patients lacking IgG/IgG4 and/or the known specific autoantibodies.

### WHAT IS NEW HERE

- ✓ Expression profiling at theRNA and protein level shows distinct patterns in pancreatic tissue from AIP patients.
- ✓ AIP patients are characterized by a very low expression of pancreatic enzymes such as trypsin, and by a concomitant loss of acinar cells.
- ✓ Identical findings are observed in a mouse model of AIP.
- ✓ AIP patients have autoantibodies against both anionic and cationic trypsinogens in high titers that may be of diagnostic usefulness.

## REFERENCES

1. Finkelberg DL, Sahani D, Deshpande V *et al.* Autoimmune pancreatitis. N Engl J Med 2006;355:2670–6.
2. Pickartz T, Mayerle J, Lerch MM. Autoimmune pancreatitis. Nat Clin Pract Gastroenterol Hepatol 2007;4:314–23.
3. Gardner TB, Levy MJ, Takahashi N *et al.* Misdiagnosis of autoimmune pancreatitis: a caution to clinicians. Am J Gastroenterol 2009;104:1620–3.
4. Yoshida K, Toki F, Takeuchi T *et al.* Chronic pancreatitis caused by an autoimmune abnormality. Proposal of the concept of autoimmune pancreatitis. Dig Dis Sci 1995;40:1561–8.
5. Zamboni G, Luttges J, Capelli P *et al.* Histopathological features of diagnostic and clinical relevance in autoimmune pancreatitis: a study on 53 resection specimens and 9 biopsy specimens. Virchows Arch 2004;445:552–63.
6. Deshpande V, Chicano S, Finkelberg D *et al.* Autoimmune pancreatitis: a systemic immune complex mediated disease. Am J Surg Pathol 2006;30:1537–45.
7. Chari ST, Smyrk TC, Levy MJ *et al.* Diagnosis of autoimmune pancreatitis: the Mayo Clinic experience. Clin Gastroenterol Hepatol 2006;4:1010–6; quiz 934.
8. Okazaki K, Uchida K, Ohana M *et al.* Autoimmune-related pancreatitis is associated with autoantibodies and a Th1/Th2-type cellular immune response. Gastroenterology 2000;118:573–81.
9. Taniguchi T, Okazaki K, Okamoto M *et al.* High prevalence of autoantibodies against carbonic anhydrase II and lactoferrin in type 1 diabetes: concept of autoimmune exocrinopathy and endocrinopathy of the pancreas. Pancreas 2003;27:26–30.
10. Moon SH, Kim MH, Park DH *et al.* Is a 2-week steroid trial after initial negative investigation for malignancy useful in differentiating autoimmune pancreatitis from pancreatic cancer? A prospective outcome study. Gut 2008;57:1704–12.
11. Church NI, Pereira SP, Deheragoda MG *et al.* Autoimmune pancreatitis: clinical and radiological features and objective response to steroid therapy in a UK series. Am J Gastroenterol 2007;102:2417–25.
12. Uchida K, Okazaki K, Nishi T *et al.* Experimental immune-mediated pancreatitis in neonatally thymectomized mice immunized with carbonic anhydrase II and lactoferrin. Lab Invest 2002;82:411–24.
13. Sarles H, Sarles JC, Muratore R *et al.* Chronic inflammatory sclerosis of the pancreas--an autonomous pancreatic disease? Am J Dig Dis 1961;6:688–98.
14. Hamano H, Kawa S, Horiuchi A *et al.* High serum IgG4 concentrations in patients with sclerosing pancreatitis. N Engl J Med 2001;344:732–8.

15. Song TJ, Kim MH, Moon SH *et al.* The combined measurement of total serum IgG and IgG4 may increase diagnostic sensitivity for autoimmune pancreatitis without sacrificing specificity, compared with IgG4 alone. Am J Gastroenterol 2009 (e-pub ahead of print).
16. Aoki S, Nakazawa T, Ohara H *et al.* Immunohistochemical study of autoimmune pancreatitis using anti-IgG4 antibody and patients' sera. Histopathology 2005;47:147–58.
17. Watanabe S, Suzuki K, Kawauchi Y *et al.* Kinetic analysis of the development of pancreatic lesions in mice infected with a murine retrovirus. Clin Immunol 2003;109:212–23.
18. Detlefsen S, Mohr Drewes A, Vyberg M *et al.* Diagnosis of autoimmune pancreatitis by core needle biopsy: application of six microscopic criteria. Virchows Arch 2009;454:531–9.
19. Rossi L, Serafini S, Franchetti P *et al.* Inhibition of murine AIDS by a heterodinucleotide of azidothymidine and 9-(R)-2-(phosphonomethoxypropyl)adenine. J Antimicrob Chemother 2002;50:639–47.
20. Huber W, von Heydebreck A, Sultmann H *et al.* Variance stabilization applied to microarray data calibration and to the quantification of differential expression. Bioinformatics 2002;18 (Suppl 1): S96–104.
21. Tusher VG, Tibshirani R, Chu G. Significance analysis of microarrays applied to the ionizing radiation response. Proc Natl Acad Sci USA 2001;98:5116–21.
22. Kaufman L, Rousseeuw PJ. Findings Groups in Data—An Introduction to Cluster Analysis. John Wiley & Sons: London, 2005.
23. Dennis G Jr, Sherman BT, Hosack DA *et al.* DAVID: database for annotation, visualization, and integrated discovery. Genome Biol 2003;4:P3.
24. Klose J. Fractionated extraction of total tissue proteins from mouse and human for 2-D electrophoresis. Methods Mol Biol 1999;112:67–85.
25. Wandschneider S, Fehring V, Jacobs-Emeis S *et al.* Autoimmune pancreatic disease: preparation of pancreatic juice for proteome analysis. Electrophoresis 2001;22:4383–90.
26. Mortz E, Krogh TN, Vorum H *et al.* Improved silver staining protocols for high sensitivity protein identification using matrix-assisted laser desorption/ionization-time of flight analysis. Proteomics 2001;1:1359–63.
27. Hellman U, Wernstedt C, Gonez J *et al.* Improvement of an "In-Gel" digestion procedure for the micropreparation of internal protein fragments for amino acid sequencing. Anal Biochem 1995;224:451–5.
28. Löhr M, Müller P, Schmidt C *et al.* Immortalized bovine pancreatic duct cells become tumorigenic after transfection with mutant k-ras. Virchows Arch 2001;438:581–90.
29. Krüger B, Emmrich J, Tessenow W *et al.* Anionic and cationic trypsin(ogen)-like immunoreactivity in the diagnosis of acute pancreatitis [abstr]. Clin Biochem Rev 1993;14:207.
30. Sahin-Toth M. Human cationic trypsinogen. Role of Asn-21 in zymogen activation and implications in hereditary pancreatitis. J Biol Chem 2000;275:22750–5.
31. Kukor Z, Toth M, Sahin-Toth M. Human anionic trypsinogen: properties of autocatalytic activation and degradation and implications in pancreatic diseases. Eur J Biochem 2003;270:2047–58.
32. Szmola R, Kukor Z, Sahin-Toth M. Human mesotrypsin is a unique digestive protease specialized for the degradation of trypsin inhibitors. J Biol Chem 2003;278:48580–9.
33. Wartmann T, Kähne T, Schulz HU *et al.* Proteolytic cleavage and inactivation of human pancreatic secretory trypsin inhibitor (SPINK1) by cathepsin B. Gastroenterology 2006;130 (Suppl. 2): A–59.
34. Kojima M, Sipos B, Klapper W *et al.* Autoimmune pancreatitis: frequency, IgG4 expression, and clonality of T and B cells. Am J Surg Pathol 2007;31:521–8.
35. Sugumar A, Kloppel G, Chari ST. Autoimmune pancreatitis: pathologic subtypes and their implications for its diagnosis. Am J Gastroenterol 2009;104:2308–10; quiz 2311.
36. Schnekenburger J, Schick V, Kruger B *et al.* The calcium binding protein S100A9 is essential for pancreatic leukocyte infiltration and induces disruption of cell-cell contacts. J Cell Physiol 2008;216:558–67.
37. Lord PW, Stevens RD, Brass A *et al.* Investigating semantic similarity measures across the Gene Ontology: the relationship between sequence and annotation. Bioinformatics 2003;19:1275–83.
38. Brors B. Microarray annotation and biological information on function. Methods Inf Med 2005;44:468–72.
39. Weiss FU, Halangk W, Lerch MM. New advances in pancreatic cell physiology and pathophysiology. Best Pract Res Clin Gastroenterol 2008;22:3–15.
40. Rinderknecht H, Stace NH, Renner IG. Effects of chronic alcohol abuse on exocrine pancreatic secretion in man. Dig Dis Sci 1985;30:65–71.
41. Asada M, Nishio A, Uchida K *et al.* Identification of a novel autoantibody against pancreatic secretory trypsin inhibitor in patients with autoimmune pancreatitis. Pancreas 2006;33:20–6.
42. Esposito I, Born D, Bergmann F *et al.* Autoimmune pancreatocholangitis, non-autoimmune pancreatitis and primary sclerosing cholangitis: a comparative morphological and immunological analysis. PLoS ONE 2008;3:e2539.
43. Notohara K, Burgart LJ, Yadav D *et al.* Idiopathic chronic pancreatitis with periductal lymphoplasmacytic infiltration: clinicopathologic features of 35 cases. Am J Surg Pathol 2003;27:1119–27.
44. Detlefsen S, Sipos B, Zhao J *et al.* Autoimmune pancreatitis: expression and cellular source of profibrotic cytokines and their receptors. Am J Surg Pathol 2008;32:986–95.
45. Vasseur S, Folch-Puy E, Hlouschek V *et al.* p8 improves pancreatic response to acute pancreatitis by enhancing the expression of the anti-inflammatory protein pancreatitis-associated protein I. J Biol Chem 2004;279:7199–207.
46. Kamisawa T, Yoshiike M, Egawa N *et al.* Treating patients with autoimmune pancreatitis: results from a long-term follow-up study. Pancreatology 2005;5:234–8; discussion 238–40.
47. Chandan VS, Iacobuzio-Donahue C, Abraham SC. Patchy distribution of pathologic abnormalities in autoimmune pancreatitis: implications for preoperative diagnosis. Am J Surg Pathol 2008;32:1762–9.
48. Kloppel G, Detlefsen S, Feyerabend B. Fibrosis of the pancreas: the initial tissue damage and the resulting pattern. Virchows Arch 2004;445:1–8.
49. Frulloni L, Lunardi C, Simone R *et al.* Identification of a novel antibody associated with autoimmune pancreatitis. N Engl J Med 2009;361:2135–42.
50. Guarneri F, Guarneri C, Benvenga S. Helicobacter pylori and autoimmune pancreatitis: role of carbonic anhydrase via molecular mimicry? J Cell Mol Med 2005;9:741–4.
51. Jesnowski R, Isaksson B, Möhrcke C *et al.* Helicobacter pylori in autoimmune pancreatitis and pancreatic carcinoma. Pancreatology 2010;10 (in press).